University of Bath

Alternative formats
If you require this document in an alternative format, please contact:
openaccess@bath.ac.uk

ACCOUNTS
of chemical research

Prediction of Electron Energies in Metal Oxides

ARON WALSH* AND KEITH T. BUTLER

*Centre for Sustainable Chemical Technologies and Department of Chemistry,
University of Bath, Bath BA2 7AY, U.K.*

CONSPECTUS

The ability to predict energy levels in metal oxides is paramount to developing useful materials, such as in the development of water photolysis catalysts and efficient photovoltaic cells. The binding energy of electrons in materials encompasses a wealth of information concerning their physicochemistry. The energies control the optical and electrical properties, dictating for which kinds of chemistry and physics a particular material is useful. Scientists have developed theories and models for electron energies in a variety of chemical systems over the past century. However, the prediction of quantitative energy levels in new materials remains a major challenge. This issue is of particular importance in metal oxide research, where novel chemistries have opened the possibility of a wide range of tailored systems with applications in important fields including light-emitting diodes, energy efficient glasses, and solar cells.
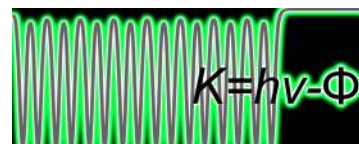
In this Account, we discuss the application of atomistic modeling techniques, covering the spectrum from classical to quantum descriptions, to explore the alignment of electron energies between materials. We present a number of paradigmatic examples, including a series of oxides (ZnO, In_2O_3, and Cu_2O). Such calculations allow the determination of a "band alignment diagram" between different materials and can facilitate the prediction of the optimal chemical composition of an oxide for use in a given application.

Throughout this Account, we consider direct computational solutions in the context of heuristic models, which are used to relate the fundamental theory to experimental observations. We review a number of techniques that have been commonly applied in the study of electron energies in solids. These models have arisen from different answers to the same basic question, coming from solid-state chemistry and physics perspectives. We highlight common factors, as well as providing a critical appraisal of the strengths and weaknesses of each, emphasizing the difficulties in translating concepts from molecular to solid-state systems.

Finally, we stress the need for a universal description of the alignment of band energies for materials design from first-principles. By demonstrating the applicability and challenges of using theory to calculate the relevant quantities, as well as impressing the necessity of a clarification and unification of the descriptions, we hope to provide a stimulus for the continued development of this field.

Introduction

The importance of electron energies in the solid-state has been recognized for the past century.[1] While the relative position of electronic bands in materials determines what optical transitions can occur, the absolute energies of these bands control what chemistry and physics can take place. For example, the energy of the valence band in a semiconductor can determine whether it has sufficient oxidative power to generate O_2 for the photolysis of water,[2] as can the energy of the conduction band influence the kinetics of electron transfer in a photovoltaic cell.[3] Many theories and models have been developed to describe the electronic behavior of different classes of chemical system, but the reliable calculation of electron energies, in particular for newly discovered or predicted materials, remains a major challenge.

The challenge for computational chemistry is twofold, first to provide the correct electronic energy levels within a given material and then to compare the levels between materials for purposes of designing systems and devices.

For molecules and other finite systems, the energies associated with electron removal (ionization potential, IP) and addition (electron affinity, EA) are well-defined quantities, which can be given with respect to an absolute vacuum level (the energy of an electron in perfect vacuum), as illustrated in Figure 1. The chemical utility of these quantities is wide-ranging, for example,

- the difference between electron addition and removal energies defines the fundamental band gap, $E_g = IP - EA$,
- the mean of electron removal and addition is the Mulliken electronegativity (χ), $\chi = (IP + EA)/2$,[4]
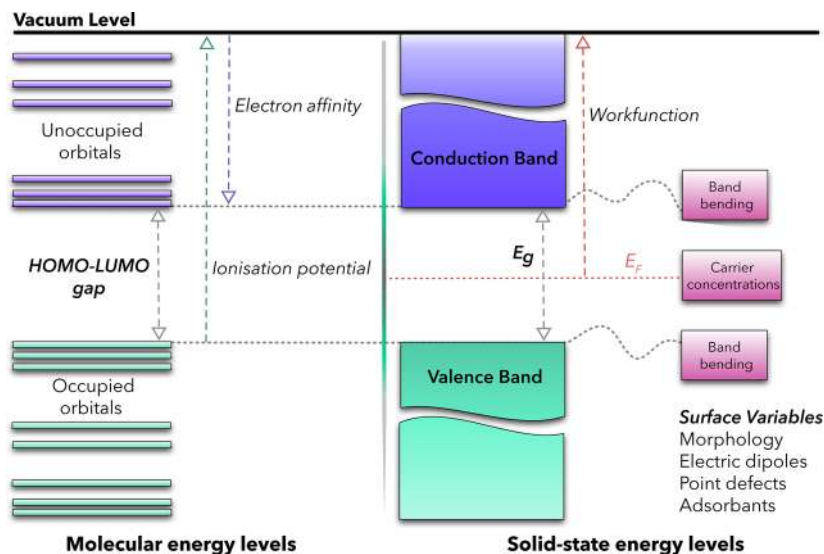
FIGURE 1. Electronic descriptions of molecular and solid systems. Values in the solid state are poorly defined on an absolute scale, due to a number of factors; some sources of discrepancy are listed to the right-hand side. E_g represents the band gap and E_F the Fermi level.

- the negative of the mean defines the electron chemical potential, that is, $\mu = -\chi$, from the central difference of $(\partial E/\partial N)_Z$, where N and Z represent the number of electrons and the nuclear coordinates, respectively,[5]
- the chemical hardness is equivalent to half the value of the band gap, that is, $(IP - EA)/2$, from the central difference of $1/2(\partial^2 E/\partial N^2)_Z$.[6]

In the solid-state, electron binding energies are notoriously difficult to evaluate experimentally, theoretically, or computationally. Furthermore, for semiconducting or metallic materials, we introduce an additional potential, the workfunction (Φ), which is the energy to remove an electron from the Fermi level (E_F, determined by the electron and hole carrier concentrations in the solid) to the vacuum level. These various quantities are illustrated in Figure 1.

Each measurement technique of interest, including thermionic, electrochemical, optical, and photoemission spectroscopies, contains an implicit dependence on the crystallographic orientation and surface morphology of the sample.[7] As stated by Henrich and Cox,[7] "The workfunction is an extremely sensitive measure of the state of a surface. In fact it is so sensitive for metal oxides that its absolute value has little significance". Surface dipoles have a direct influence on the position of the local vacuum level; electrical carrier concentrations determine E_F, and the densities of point defects and surface adsorbents can cause significant changes to both. Band bending at semiconductor surfaces and interfaces is rarely negligible.[8] Nonetheless, the surface workfunction is a quantity that is regularly measured and reported. For

example, the workfunction of ZnO has been measured between 3 and 6 eV depending on the experimental conditions.[7] For ZnO thin films, it has been demonstrated that the workfunction is tunable over a large range, depending on the partial pressure of oxygen during synthesis.[9]

In the solid-state, concepts such as workfunction and Fermi level are central to theories and descriptions of electronic device functionality. Although these concepts are not widely used in the materials chemistry community, they are routinely and successfully applied in device design involving traditional semiconducting materials. As oxides become increasingly employed in electronic devices, it is important that such concepts be clarified in the context of oxide systems, where the values involved are sensitive to several physical parameters. In this Account, we discuss the chemical origin of these quantities and the range of methods available to calculate them.

Theoretical Approaches

Atomistic materials modeling techniques have become increasingly predictive,[10] offering the possibility of calculating electronic structures accurate enough to be used in large-scale models and device design. Many theoretical approaches for describing the binding energy of electrons in oxides have been developed to varying degrees of success and generality. For example, by 1940, Mott and Gurney had presented a semiempirical approach based upon the variations in the electrostatic potential in heteropolar solids, which avoids the anisotropy of an electron leaving the

crystal: the measured ionization potentials of the isolated atoms modified by the calculated Madelung potential of the solid.[1]

Based on first-principles electronic structure techniques, such as density functional theory (DFT), there are several approaches to calculate the relevant quantities, which can be broadly separated into three areas:

(1) Surface models: A material is represented as a semi-infinite slab repeating in two dimensions, with a surface to vacuum in the third. Formally, 2D or 3D boundary conditions can be employed, or alternatively a multiregion embedding procedure can be adopted.[11] Irrespective of the physical model, the value of the electrostatic potential in the vacuum region is used to align the single- or quasi-particle electron energies. The surface orientation dependence encountered in experiments is also important in these models. Nonetheless, single surface terminations have been used to predict defect levels,[12] band edge potentials,[13] and band alignments.[14] An additional issue is exactly how to model the surface, whether to chemically passivate dangling bonds and whether to relax the surface coordinates. Different models can lead to very different values, on the order of electronvolts, being calculated.

(2) Interface models: Approaches for heterostructure alignments, similar to the methods used for alignment of X-ray photoemission spectra,[15−17] have shown good agreement with experiment for tetrahedral semiconductors.[18,19] Such models rely on a reference potential (either the averaged electrostatic potential or a localized core state); a general scheme is presented in Figure 2. The main issues are that the alignment is produced on a relative scale, with an implicit assumption of transitivity, and the extension to more complex systems (structures) remains ill-defined. However, the calculation of semiconductor/oxide interfaces, in good agreement with experiment, has been demonstrated.[20] For solid/liquid interfaces (e.g., in photocatalytic water-splitting) calculation of workfunctions requires the sampling of a large number of configurations.[13] Due to the associated computational expense, a number of approximations are common, for example, thin slab models, reduced k-point sampling, and the use of low-quality basis sets. We emphasize the difference between the alignment calculated for a particular heterostructure, including all interfacial effects,[21] and the "natural" alignment of the respective bulk energy levels,[18,22,23] which aims to exclude these effects. Clearly, the band alignment between two materials will depend strongly on the type of termination at the interface, either by different crystallographic planes or a different chemical structure.
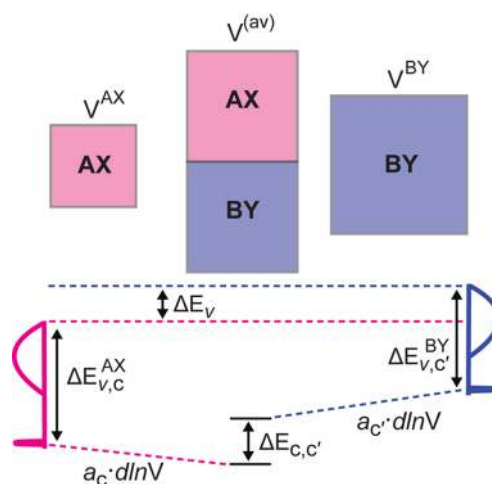

FIGURE 2. A valence band alignment technique using core levels (e.g., O 1s states). The materials AX and BY are combined to form an AX|BY heterostructure, with the difference in core levels ($\Delta E_{c,c'}$) used to align the valence bands of the isolated materials. A second-order correction accounts for the core-level shift due to the volume change from the isolated crystals (V^{AX}, V^{BY}) to the heterostructure (V^{av}) based on the core-level deformation potential (a_c). See ref 18 for further details.

(3) Reaction energies: Electronic structure approaches such as DFT are well suited to calculating total energies in addition to one-electron energies of materials.[24−26] This strength has been exploited to calculate alignments at solid/water interfaces.[27,28] These methods involve inserting an electron into the electrode material and a proton into the liquid phase; the free energy change provides a direct estimate of the line-up with respect to the standard hydrogen electrode. Similarly Chen and Wang[29] predicted the redox energies for a range of semiconductors by calculating each term of the associated thermodynamic cycle, an approach developed by Gerischer for assessing the corrosion of metal oxides and sulfides.[30,31]

A final technique worth briefly mentioning is model-solid theory, which has been used to align the band structure of a periodic solid to the vacuum level using the neutral atoms as a reference.[32] While the approach proved useful when applied to some semiconductors, for oxides, the variation in charge states and environments makes it difficult to generalize.

The above methods have been applied using the standard local density approximation (LDA) and generalized gradient approximation (GGA) levels of DFT for a number of years. However, when quantitative results are required, based on electronic structure calculations, it is often necessary to go beyond these approximations, which grossly underestimate the band gaps of semiconductors and insulators.[33,34] Methods for achieving quantitatively accurate band structures, such as nonlocal hybrid functionals[35−39] or many-body
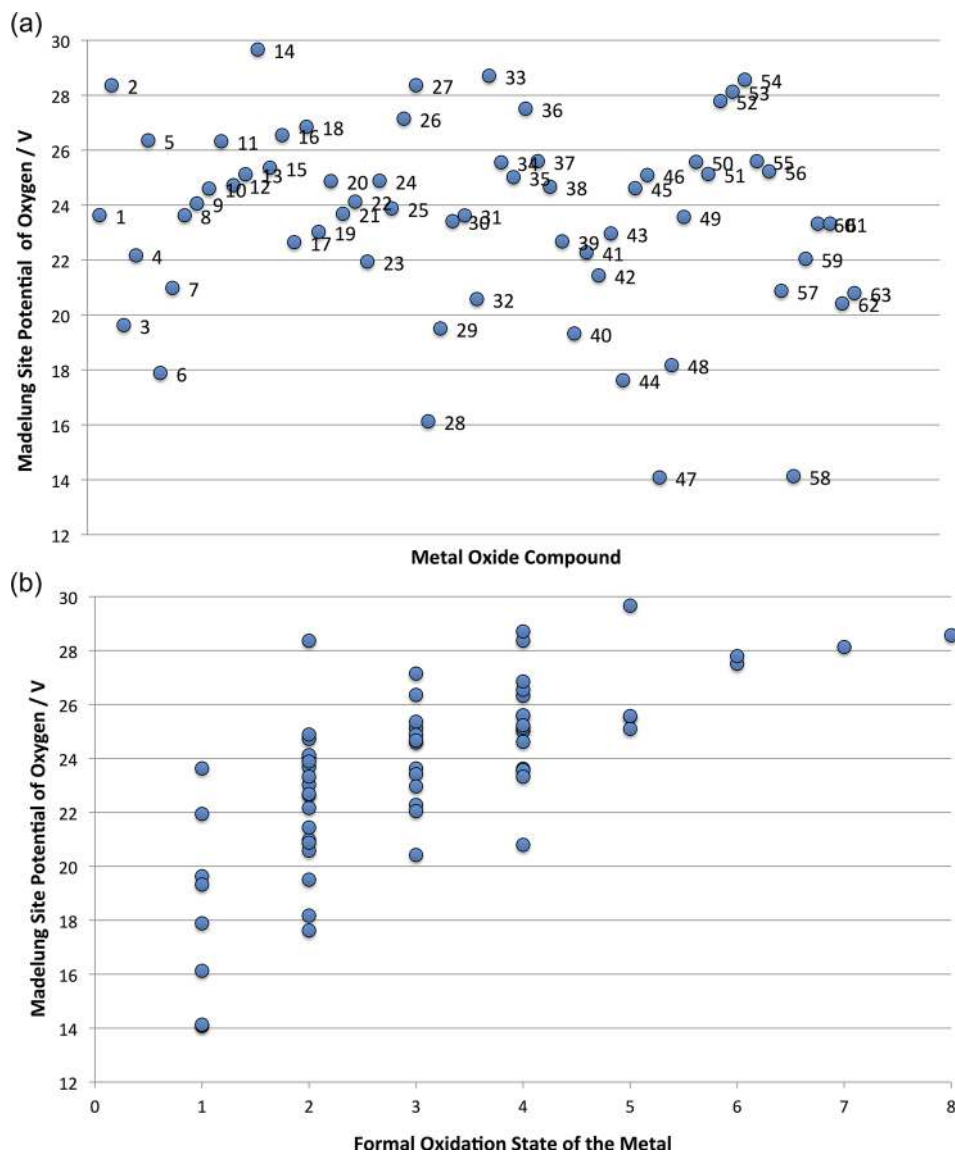
FIGURE 3. (a) Average electrostatic environment of the oxygen lattice site across the binary oxides from Li_2O (1) to PoO_2 (63) within the point charge approximation. (b) The distribution of environments as a function of the oxidation state of the metal is shown, with the lowest value calculated for Cs_2O (14.08 V) and the highest for V_2O_5 (29.67 V).

perturbation theory (e.g., the *GW* approximation[40]) are more demanding in terms of computational expense, again often necessitating approximations in the models that may introduce spurious errors of unknown magnitude.

We now consider theoretical frameworks for predicting band energies and alignments, which are less rigorous than a full quantum mechanical treatment but also less demanding on computational resources. The first originates from solid-state chemistry and the others from physics; although, they all address the same issue:

(1) Mulliken electronegativity has been applied to assess the band alignment problem following "Anderson's rule", that is, the alignment of vacuum levels for two or more materials in contact. The effective electronegativity of the materials can be used to construct a heterostructure band diagram.[41] In 1974, Nethercot[42] proposed the "geometric mean of electronegativities" to predict the work functions of II−VI, III−V, and metal halide materials in agreement with experiments. This approach was then applied by Bulter and Ginley to a range of oxide materials[43] and extended by Xu and Schoonen to assess the band energies of over 50 semiconductors.[44] Despite its conceptual simplicity, the method produces electron energies in reasonably quantitative agreement with experiment. Recently it has been successful in the high-throughput screening of perovskites for light capture[45] and the electronic structure analysis of new
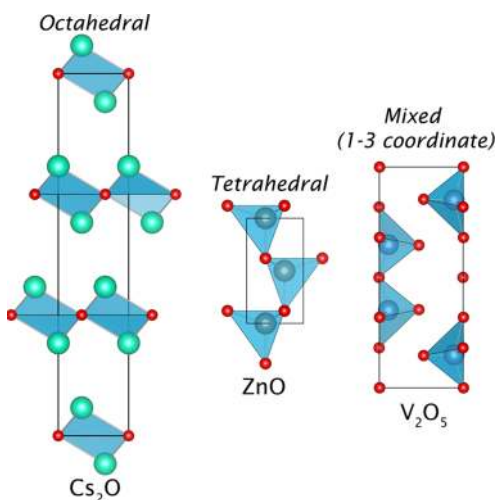
FIGURE 4. Crystal structures of Cs_2O (anti-$CdCl_2$ lattice), ZnO (wurtzite), and V_2O_5 (shcherbinaite) illustrating the diversity in the oxygen coordination environments (red spheres).

ns^2 lone pair materials.[46] However, the method is based solely on chemical composition and cannot account for the effects of bonding or crystal structure. Within this approximation, all polymorphs and polytypes of a material have equivalent electron energies.

(2) The common anion rule is again related to "Anderson's rule", with the energies computed using a tight-binding model. It can be employed to predict the valence band positions of tetrahedral semiconductors using anion p orbital energies and bond lengths. It has given good agreement with experiment for energy alignments of some II−VI and oxide semiconductors;[47] however, in general the approximation fails due to a combination interface dipoles and the participation of metal d orbitals in bonding. As discussed below, the large variety of coordination environments makes it difficult to apply to metal oxides.
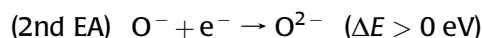
(3) Charge neutrality level (CNL) arises from the metal-induced gap-state description of metal−semiconductor interfaces.[48,49] It is sometimes termed a "branch-point energy" or "point of zero charge" and is related to the midgap energy integrated across the first Brillouin zone.[50] The CNLs for a wide range of semiconductors have been calculated using a tight-binding model,[51] and values have also been reported for more complex oxides.[52,53] The approach can be extended to specific heterojunctions by including the electronegativity of the materials in order to account for charge transfer induced dipoles at the interface.[54] It should be noted that while the Mulliken approximation provides an absolute midgap energy relative to the vacuum, for periodic DFT calculations the CNL is only defined relative to an arbitrary reference potential.[55] In addition it has been suggested by Klein that

oxide interfaces are not controlled by gap states,[56] which is also consistent with the behavior of amorphous oxides.[57]

In the following, a number of general concepts associated with the bonding in metal oxides are revisited, with a particular emphasis on their relation to the energies of electrons in materials. We consider first the representation of metal oxide systems as an ionic solid, highlighting the trends in midgap energies based on coordination and revealing the deficiencies of such a method for calculations of ionization potentials, necessitating the use of explicit electronic structure methods.

The Ionic Solid

The chemical bonding in metal oxides is predominately ionic in nature. While the distribution of charge depends on both the crystal structure and the chemical nature of the metals, the bonds are unambiguously heteropolar.[58,59] To calculate the lattice energy of an ionic solid, it is standard to consider a thermochemical cycle (e.g., the Born−Haber cycle); however, for oxides, the second electron affinity of oxygen is ill-defined. In the gas phase, the oxide (O^{2-}) ion is not stable, that is,

$$(\text{1st EA}) \quad O + e^- \rightarrow O^- \quad (\Delta E = -1.46 \text{ eV})$$

$$(\text{2nd EA}) \quad O^- + e^- \rightarrow O^{2-} \quad (\Delta E > 0 \text{ eV})$$

In other words, the second electron is not bound *in vacuo*; the second electron affinity of oxygen is *positive*. The philosophical implications of this behavior have been discussed by Harding.[60] The practical implication is that the solid-state environment of oxygen is crucial for stabilizing the second electron to produce the diamagnetic $2p^6$ configuration. It is well-known that the valence band of metal oxides is composed predominately of O 2p orbitals; hence, the electron energies must be sensitive to the local environment. Therefore it may be possible to estimate the band structure of a metal oxide on the basis of the electrostatic environment.

Oxide Electrostatic Environment

The structural diversity of metal oxides results in a large variation in local bonding environments, which can be quantified through electrostatic (Madelung) potential. Here the potential is calculated using a simple point charge model and an Ewald summation technique, depending only on the ion charges (q_i) and the ion separations (r_{0-i}):[61]

$$V_0 = \sum_{i=1}^{N} \frac{q_i}{r_{0-i}}$$

The utility of this quantity is well documented, for example, explaining hole conductivity in high T_C superconductors[62] and the surface defect behavior of metal oxides.[63,64] We have calculated the Madelung potential of oxygen in the most stable phase of every known binary oxide from Li_2O to PoO_2, averaging inequivalent oxide sites, with the results graphed in Figure 3 (the raw data available in an online repository[65]).

There is a striking spread of 16 V in site potentials, with a correlation between metal−oxygen separation and formal oxidation state of the metal. The weakest potential is found for a monovalent Cs_2O, while the strongest potential is pentavalent V_2O_5. Divalent metals such as ZnO are of intermediate behavior. These three materials again emphasize how the diversity of the structures, as illustrated in Figure 4, influences the electrostatic environment of the oxide ion. Cs_2O adopts the layered anti-$CdCl_2$ structure, where oxygen has an octahedral environment. The wurtzite phase of ZnO consists of oxide ions at the center of metal tetrahedra, while in V_2O_5 there are three distinct oxygen sites with coordination numbers from 1 to 3.

Based on this simple analysis, it would be expected that the ionization energies follow the same trend as the Madelung potentials, that is, $Cs_2O < ZnO < V_2O_5$. The midgap energies predicted from the Mulliken electronegativity of the compounds do follow this trend (4.05 eV > 5.95 eV > 6.12 eV); however, due to the larger band gap of ZnO, the associated ionization potentials slightly deviate (5.15 eV > 7.67 eV < 7.52 eV).

This type of classical electrostatic description does not account for the detailed electronic structure of the materials considered; thus alone it cannot predict changes in ionization energies due to differing band gaps and widths. While an extension to this approach has been developed to approximate electron and hole energies[66] and has been successful in the description of TiO_2 polymorphs,[67] the associated thermochemical cycles for metal oxides are impeded by the electron affinity of oxygen, as previously highlighted. In order to accurately account for these effects, it is necessary to augment the model to include long-range polarization or to employ explicit electronic structure techniques.

Oxide Band Energies

DFT is currently the most popular method for calculating the electronic structure of solid-state oxides. We will consider just a few paradigmatic examples of the state-of-the-art in this field, noting that such calculations of metal oxides are numerous.

Zinc Oxide. The ionization potential for a nonpolar $(11\bar{2}0)$ ZnO single-crystal surface was measured by Swank as 7.82 eV below the vacuum level.[68] There is an abundance of computations on ZnO bulk and defective crystals, nanostructures, and surfaces; however, reports of bulk electron energies are rare. One difficulty is the polar nature of the common (0001) surface of wurtzite, which undergoes complex reconstructions to quench the electric dipole. In order to provide an absolute energy reference, while properly accounting for the long-range electrostatic and dielectric response to the ionization process, a mixed quantum mechanical/molecular mechanical (QM/MM) method has been developed. The result is a multiscale representation of an infinite solid-state crystal, for example, as implemented in the ChemShell package.[69,70] A central core of the material is explicitly described using DFT and an outer region is simulated using analytical polarizable potentials, which in turn is embedded in a dielectric continuum. This type of embedded cluster approach follows the early work of Mott and Littleton[71] and avoids the orientation dependence of surface models. To calculate the electronic structure of ZnO, a hybrid functional (B97-1) has been used. Calculations by Sokol et al. place the ionization potential at 7.71 eV below the vacuum, in good agreement with experimental values. We emphasize here the explicit calculation of the electron removal energy (IP) and not the one-electron Kohn−Sham eigenvalue that is sometimes used as an approximation. Remarkably, the Mulliken model predicts an IP of 7.67 eV in very good agreement with both experiment and the QM/MM model. In contrast to the binding energy of ca. 7.7 eV, due to its n-type nature with E_F close to the conduction band, values for the workfunction of ZnO are significantly smaller: from 3 to 6 eV depending on the surface preparation procedure.[7]

Indium Sesquioxide. The band energies of In_2O_3 have gathered significant interest.[56] The nonpolar (111) surface has been found to dominate in crystalline samples.[72] Calculations of the ionization potential of this termination have been performed[73] using a hybrid DFT approach. The HSE06 functional (like B97-1) incorporates a percentage (25%) of HF electron exchange and reproduces the band gap of the bulk material.[74] However, unlike the ZnO study, a system based on periodic boundary conditions was used to represent a 2D infinite slab of a surface with no net dipole. The calculated ionization potential is 7.22 eV for the (111) surface,[73] which compares very well to the value of 7.1 eV measured for polycrystalline samples.[9] Here, the Mulliken model predicts an

IP of 6.65 eV, with an apparent error of ca. 0.5 eV. Notably from computations, other surface terminations produce variations in the potential of ± 0.7 eV. The measured ionization potentials and workfunctions of In_2O_3[75] have also been shown to fluctuate by over 1 eV by heating in air, which was attributed to surface dipole modifications with oxygen exchange. In contrast, the band alignment of In_2O_3 to CdS proves relatively robust with regards to preparatory conditions.[76]

Cuprous Oxide. Both ZnO and In_2O_3 are wide band gap n-type semiconductors. A representative p-type material is Cu_2O. The cuprite structure contains a unique arrangement of linearly coordinated Cu ions; the nonpolar (111) and polar (100) are two dominant terminations. Photoemission measurements of sputtered thin films place the ionization potential at 5.0–5.7 eV below the vacuum level, with a notable dependence on the substrate.[77] Indeed, Soon et al. have investigated the (111) surface structure of Cu_2O, using a periodic slab model as a function of the oxygen partial pressure and identified a large variation in the calculated ionization potential (4.08–5.36 eV).[78] From the Mulliken electronegativity of Cu_2O, the IP is placed at 6.43 eV, which contains the largest error of the three oxides studied owing to the unusual geometric and electronic structure of the cuprous ion. Deuermeier et al. have explicitly considered the formation of the Cu_2O/In_2O_3 interface, with a measured valence band offset in the range of 2.6–2.9 eV,[79] consistent with the electron binding energies of the isolated materials. The band alignment of Cu_2O/ZnO was recently measured as being 2.2 eV, again in good agreement with the relative IPs.[80]

Using computed or measured ionization potentials one can construct an alignment diagram by taking the vacuum level as a reference and placing the band structures accordingly. Again, this concerns an intrinsic "natural" band offset that will be dominant factor in determining the electronic properties of a given interface but does not include any specific interfacial effects. A representative diagram is shown in Figure 5, which collects data for the three oxides previously discussed and three other important semiconductors: IPs for ZnO, In_2O_3, GaN, and TiO_2 have been calculated using the QM/MM approach discussed above, while values for Cu_2O and Si are based upon experimentally measured IPs. The results are chemically intuitive in terms of the relative binding energies of different elemental components and can be useful for identifying materials combinations, for example, solid solutions for enhancing photoactivity. However, it is difficult to provide an extended alignment of oxide materials based on literature values due to the variations in both the physical models (e.g., bulk, surface or interface
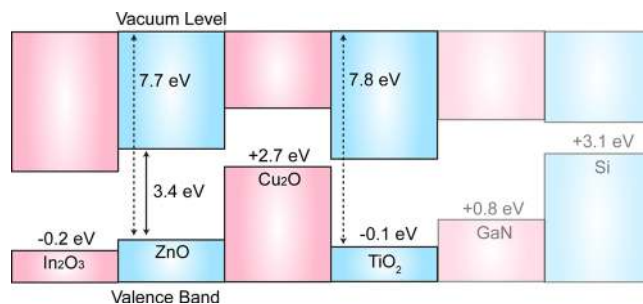

FIGURE 5. Representative valence band alignments of In_2O_3, ZnO, and Cu_2O with respect to rutile-structured TiO_2 and two popular semiconductors (GaN and Si). All values are based on ionization potentials calculated using DFT with hybrid exchange–correlation functionals, with the exception of Cu_2O and Si, which have been taken from experimental reports. Data collected from refs 67, 81, and 82.

alignments) and levels of theory (e.g., different treatments of electron correlation within DFT). Presently, studies of individual materials require substantial amounts of preparation and calculation time, so there have been few systemic studies performed. An accurate, robust, and transferable procedure for calculating electron energies in solids is urgently required.

Outlook

Despite the simplicity of the underlying concepts, both the calculation and measurement of the binding energy of electrons in solids and, in particular, metal oxides continue to pose scientific challenges. A number of approaches to compute these energies have been discussed. The ultimate aim is for the ionization potential and electron affinity of an arbitrary material (chemical structure and composition) to be predicted with good certainty. While each of the techniques mentioned have merit when applied to specific systems, there is a lack of generality with respect to absolute values. Problems relating to surface termination and structure are ubiquitous. The need for a universal and tractable approach to predict band energies in the design and optimization of novel material systems is clear, with immediate applications in solar energy conversion in photovoltaic and photoelectrochemical devices and energy storage in electrochemical batteries; it just remains to be developed and adopted by the community.

BIOGRAPHICAL INFORMATION

Aron Walsh was born in Dublin, Ireland. He was awarded his Ph.D. (with G. W. Watson) from Trinity College Dublin in 2006 for his work on the electronic structure of post-transition metal oxides. Subsequently he worked at the National Renewable Energy Laboratory (with S.-H. Wei) and University College London (with C. R. A. Catlow), before joining the University of Bath. Aron is currently a Royal Society University Research Fellow and leads a research group in computational materials chemistry.

Keith T. Butler was born in Dublin, Ireland. He obtained his Ph.D. in Computational Chemistry (with D.W. Lewis) from University College London in 2009. Subsequently, he joined the University of Sheffield (with J. H. Harding) to work as part of an EU network on silicon solar cells. Keith moved to the University of Bath in 2013 as a postdoctoral researcher in the SUPER*SOLAR* Hub, working on the theory of transparent conducting oxides.

FOOTNOTES

*E-mail: a.walsh@bath.ac.uk.

REFERENCES

1 Mott, N. F.; Gurney, R. W. *Electronic Processes in Ionic Crystals*; Oxford University Press: Oxford, 1940.

2 Grätzel, M. Photoelectrochemical cells. *Nature* **2001**, *414*, 338–344.

3 Grätzel, M. Perspectives for dye-sensitized nanocrystalline solar cells. *Prog. Photovoltaics* **2000**, *8*, 171.

4 Mulliken, R. S. A new electroaffinity scale; together with data on valence states and on valence ionization potentials and electron affinities. *J. Chem. Phys.* **1934**, *2*, 782–793.

5 Pearson, R. G. Absolute electronegativity and hardness: Application to inorganic chemistry. *Inorg. Chem.* **1988**, *27*, 734–740.

6 Parr, R. G.; Pearson, R. G. Absolute hardness: Companion parameter to absolute electronegativity. *J. Am. Chem. Soc.* **1983**, *105*, 7512–7516.

7 Henrich, V. E.; Cox, P. A. *The Surface Science of Metal Oxides*; Cambridge University Press: Cambridge, U.K., 1994.

8 Zhang, Z.; Yates, J. T. Band bending in semiconductors: Chemical and physical consequences at surfaces and interfaces. *Chem. Rev.* **2012**, *112*, 5520–5551.

9 Klein, A.; Körber, C.; Wachau, A.; Säuberlich, F.; Gassenbauer, Y.; Schafranek, R.; Harvey, S. P.; Mason, T. O. Surface potentials of magnetron sputtered transparent conducting oxides. *Thin Solid Films* **2009**, *518*, 1197–1203.

10 Catlow, C. R. A.; Guo, Z. X.; Miskufova, M.; Shevlin, S. A.; Smith, A. G. H.; Sokol, A. A.; Walsh, A.; Wilson, D. J.; Woodley, S. M. Advances in computational studies of energy materials. *Philos. Trans. R. Soc., A* **2010**, *368*, 3379–3456.

11 Inglesfield, J. E.; Benesh, G. A. Surface electronic structure: Embedded self-consistent calculations. *Phys. Rev. B* **1988**, *37*, 6682–6700.

12 West, D.; Sun, Y. Y.; Zhang, S. B. Importance of the correct Fermi energy on the calculation of defect formation energies in semiconductors. *Appl. Phys. Lett.* **2012**, *101*, No. 082105.

13 Toroker, M. C.; Kanan, D. K.; Alidoust, N.; Isseroff, L. Y.; Liao, P.; Carter, E. A. First principles scheme to evaluate band edge positions in potential transition metal oxide photocatalysts and photoelectrodes. *Phys. Chem. Chem. Phys.* **2011**, *13*, 16644–16654.

14 Höffling, B.; Schleife, A.; Rödl, C.; Bechstedt, F. Band discontinuities at Si-TCO interfaces from quasiparticle calculations: Comparison of two alignment approaches. *Phys. Rev. B* **2012**, *85*, No. 035305.

15 King, P.; Veal, T. D.; Kendrick, C. E.; Durbin, S. M.; McConville, C. F. InN/GaN valence band offset: High-resolution X-ray photoemission spectroscopy measurements. *Phys. Rev. B* **2008**, *78*, No. 033308.

16 Kowalczyk, S. P.; Cheung, J. T.; Kraut, E. A.; Grant, R. W. CdTe-HgTe (1̄11) heterojunction valence-band discontinuity: A common-anion-rule contradiction. *Phys. Rev. Lett.* **1986**, *56*, 1605–1608.

17 King, P. D. C.; Veal, T. D.; Jefferson, P. H.; McConville, C. F.; Wang, T.; Parbrook, P. J.; Lu, H.; Schaff, W. J. Valence band offset of InN/ AlN heterojunctions measured by x-ray photoelectron spectroscopy. *Appl. Phys. Lett.* **2007**, *90*, No. 132105.

18 Li, Y.-H.; Walsh, A.; Chen, S.; Yin, W.-J.; Yang, J.-H.; Li, J.; Da Silva, J. L. F.; Gong, X. G.; Wei, S.-H. Revised ab initio natural band offsets of all group IV, II-VI, and III-V semiconductors. *Appl. Phys. Lett.* **2009**, *94*, No. 212109.

19 Wei, S.-H.; Zunger, A. Valence band splittings and band offsets of AlN, GaN, and InN. *Appl. Phys. Lett.* **1996**, *69*, 2719–2721.

20 Alkauskas, A.; Broqvist, P.; Devynck, F.; Pasquarello, A. Band offsets at semiconductor-oxide interfaces from hybrid density-functional calculations. *Phys. Rev. Lett.* **2008**, *101*, No. 106802.

21 Li, Y. H.; Gong, X. G.; Wei, S.-H. Ab initio all-electron calculation of absolute volume deformation potentials of IV-IV, III-V, and II-VI semiconductors: The chemical trends. *Phys. Rev. B* **2006**, *73*, No. 245206.

22 Wei, S. H.; Zunger, A. Calculated natural band offsets of all II—VI and III—V semiconductors: Chemical trends and the role of cation d orbitals. *Appl. Phys. Lett.* **1998**, *72*, 2011–2013.

23 Van de Walle, C. G.; Neugebauer, J. Small valence-band offsets at GaN/InGaN heterojunctions. *Appl. Phys. Lett.* **1997**, *70*, 2577–2579.

24 Alfe, D.; De Wijs, G.; Kresse, G.; Gillan, M. Recent developments in ab initio thermodynamics. *Int. J. Quantum Chem.* **2000**, *77*, 871–879.

25 Lany, S. Semiconductor thermochemistry in density functional calculations. *Phys. Rev. B* **2008**, *78*, No. 245207.

26 Reuter, K.; Scheffler, M. First-principles atomistic thermodynamics for oxidation catalysis: surface phase diagrams and catalytically interesting regions. *Phys. Rev. Lett.* **2003**, *90*, No. 046103.

27 Cheng, J.; Sprik, M. Alignment of electronic energy levels at electrochemical interfaces. *Phys. Chem. Chem. Phys.* **2012**, *14*, 11245–11267.

28 Rossmeisl, J.; Qu, Z.-W.; Zhu, H.; Kroes, G.-J.; Nørskov, J. K. Electrolysis of water on oxide surfaces. *J. Electroanal. Chem.* **2007**, *607*, 83–89.

29 Chen, S.; Wang, L.-W. Thermodynamic oxidation and reduction potentials of photocatalytic semiconductors in aqueous solution. *Chem. Mater.* **2012**, *24*, 3659–3666.

30 Gerischer, H. Electrolytic decomposition and photodecomposition of compound semiconductors in contact with electrolytes. *J. Vac. Sci. Technol.* **1978**, *15*, 1422–1428.

31 Gerischer, H. On the stability of semiconductor electrodes against photodecomposition. *J. Electroanal. Chem. Interfacial Electrochem.* **1977**, *82*, 133–143.

32 Van de Walle, C. G. Band lineups and deformation potentials in the model-solid theory. *Phys. Rev. B* **1989**, *39*, 1871–1883.

33 Perdew, J. P.; Levy, M. Physical Content of the Exact Kohn-Sham Orbital Energies: Band Gaps and Derivative Discontinuities. *Phys. Rev. Lett.* **1983**, *51*, 1884–1887.

34 Sham, L. J.; Schlüter, M. Density-Functional Theory of the Energy Gap. *Phys. Rev. Lett.* **1983**, *51*, 1888–1891.

35 Marsman, M.; Paier, J.; Stroppa, A.; Kresse, G. Hybrid functionals applied to extended systems. *J. Phys.: Condens. Matter* **2008**, *20*, No. 064201.

36 Paier, J.; Marsman, M.; Kresse, G. Why does the B3LYP hybrid functional fail for metals? *J. Chem. Phys.* **2007**, *127*, No. 024103.

37 Paier, J.; Marsman, M.; Hummer, K.; Kresse, G.; Gerber, I. C.; Ángyán, J. G. Screened hybrid density functionals applied to solids. *J. Chem. Phys.* **2006**, *124*, No. 154709.

38 Hummer, K.; Harl, J.; Kresse, G. Heyd-Scuseria-Ernzerhof hybrid functional for calculating the lattice dynamics of semiconductors. *Phys. Rev. B* **2009**, *80*, No. 115205.

39 Heyd, J.; Scuseria, G. E. Efficient hybrid density functional calculations in solids: Assessment of the Heyd--Scuseria--Ernzerhof screened Coulomb hybrid functional. *J. Chem. Phys.* **2004**, *121*, 1187–1192.

40 Hedin, L. New Method for Calculating the One-Particle Green's Function with Application to the Electron-Gas Problem. *Phys. Rev.* **1965**, *139*, A796–A823.

41 Anderson, R. Germanium-Gallium Arsenide Heterojunctions. *IBM J. Res. Dev.* **1960**, *4*, 283–287.

42 Nethercot, A. H. Prediction of Fermi Energies and Photoelectric Thresholds Based on Electronegativity Concepts. *Phys. Rev. Lett.* **1974**, *33*, 1088–1091.

43 Butler, M. A.; Ginley, D. S. Prediction of Flatband Potentials at Semiconductor-Electrolyte Interfaces from Atomic Electronegativities. *J. Electrochem. Soc.* **1978**, *125*, 228–232.

44 Xu, Y.; Schoonen, M. A. A. The absolute energy positions of conduction and valence bands of selected semiconducting minerals. *Am. Mineral.* **2000**, *85*, 543–556.

45 Castelli, I. E.; Olsen, T.; Datta, S.; Landis, D. D.; Dahl, S.; Thygesen, K. S.; Jacobsen, K. W. Computational screening of perovskite metal oxides for optimal solar light capture. *Energy Environ. Sci.* **2012**, *5*, 5814–5819.

46 Burton, L. A.; Walsh, A. A photoactive titanate with a stereochemically active Sn lone pair: Electronic and crystal structure of Sn_2TiO_4 from computational chemistry. *J. Solid State Chem.* **2012**, *196*, 157–160.

47 Klein, A. Energy band alignment at interfaces of semiconducting oxides: A review of experimental determination using photoelectron spectroscopy and comparison with theoretical predictions by the electron affinity rule, charge neutrality levels, and the common anion rule. *Thin Solid Films* **2012**, *520*, 3721–3728.

48 Tersoff, J. Schottky barrier heights and the continuum of gap states. *Phys. Rev. Lett.* **1984**, *52*, 465–468.

49 Heine, V. Theory of surface states. *Phys. Rev.* **1965**, *138*, A1689–A1696.

50 Cardona, M.; Christensen, N. E. Acoustic deformation potentials and heterostructure band offsets in semiconductors. *Phys. Rev. B* **1987**, *35*, 6182–6194.

51 Monch, W. Empirical tight-binding calculation of the branch-point energy of the continuum of interface-induced gap states. *J. Appl. Phys.* **1996**, *80*, 5076–5082.

52 Robertson, J. Band offsets of wide-band-gap oxides and implications for future electronic devices. *J. Vac. Sci. Technol. B* **2000**, *18*, 1785–1791.

53 Schleife, A.; Fuchs, F.; Rodl, C.; Furthmuller, J.; Bechstedt, F. Branch-point energies and band discontinuities of III-nitrides and III-/II-oxides from quasiparticle band-structure calculations. *Appl. Phys. Lett.* **2009**, *94*, No. 012104.

54 Monch, W. Branch-point energies and the band-structure lineup at Schottky contacts and heterostrucures. *J. Appl. Phys.* **2011**, *109*, No. 113724.

55 J Ihm, A. Z.; Cohen, M. L. Momentum-space formalism for the total energy of solids. *J. Phys.: Condens. Matter* **1979**, *12*, 4409–4422.

56 Klein, A. Transparent conducting oxides: Electronic structure—property relationship from photoelectron spectroscopy with in situ sample preparation. *J. Am. Ceram. Soc.* **2012**, *96*, 331–345.

57 Deng, H.-X.; Wei, S.-H.; Li, S.-S.; Li, J.; Walsh, A. Electronic origin of the conductivity imbalance between covalent and ionic amorphous semiconductors. *Phys. Rev. B* **2013**, *87*, No. 125203.

58 Catlow, C. R. A.; Stoneham, A. M. Ionicity in solids. *J. Phys.: Condens. Matter* **1983**, *16*, 4321–4338.

59 Jansen, M.; Wedig, U. A piece of the picture - misunderstanding of chemical concepts. *Angew. Chem., Int. Ed.* **2008**, *47*, 10026–10029.

60 Harding, J. H.; Pyper, N. C. The meaning of the oxygen second-electron affinity and oxide potential models. *Philos. Mag. Lett.* **1995**, *71*, 113–121.

61 Gale, J. D.; Rohl, A. L. The general utility lattice program. *Mol. Simul.* **2003**, *29*, 291–341.

62 Torrance, J. B.; Metzger, R. M. Role of the Madelung energy in hole conductivity in copper oxides: Difference between semiconductors and high-T_C superconductors. *Phys. Rev. Lett.* **1989**, *63*, 1515–1518.

63 Walsh, A. Surface oxygen vacancy origin of electron accumulation in indium oxide. *Appl. Phys. Lett.* **2011**, *98*, No. 261910.

64 Duffy, D. M.; Hoare, J. P.; Tasker, P. W. Vacancy formation energies near the surface of an ionic crystal. *J. Phys.: Condens. Matter* **1984**, *17*, L195–L200.

65 https://github.com/WMD-Bath/Oxide-Electrostatics

66 Catlow, C. R. A.; Muxworthy, D. G. The electronic structure of divalent transition metal oxides. *Philos. Mag. B* **1978**, *37*, 63–71.

67 Scanlon, D. O; Dunnill, C. W.; Buckeridge, J.; Shevlin, S. A.; Logsdail, A. J.; Woodley, S. M.; Catlow, C. R. A.; Powell, M. J.; Palgrave, R. G.; Parkin, I. P.; Watson, G. W.; Keal, T. W.; Sherwood, P.; Walsh, A.; Sokol, A. A. Band alignment of rutile and anatase TiO$_2$. *Nat. Mater.* **2013**, *12*, 798–801.

68 Swank, R. K. Surface properties of II-VI compounds. *Phys. Rev.* **1967**, *153*, 844–849.

69 Sokol, A. A.; Bromley, S. T.; French, S. A.; Catlow, C. R. A.; Sherwood, P. Hybrid QM/MM embedding approach for the treatment of localized surface states in ionic materials. *Int. J. Quantum Chem.* **2004**, *99*, 695–712.

70 Sherwood, P .; de Vries, A. H.; Guest, M. F.; Schreckenbach, G.; Catlow, C. R. A.; French, S. A.; Sokol, A. A.; Bromley, S. T.; Thiel, W.; Turner, A. J.; Billeter, S.; Terstegen, F.; Thiel, S.; Kendrick, J.; Rogers, S. C.; Casci, J.; Watson, M.; King, F.; Karlsen, E.; Sjøvoll, M.; Fahmi, A.; Schäfer, A.; Lennartz, C. QUASI: A general purpose implementation of the QM/MM approach and its application to problems in catalysis. *J. Mol. Struct.* **2003**, *632*, 1–28.

71 Mott, N. F.; Littleton, M. J. Conduction in polar crystals. I. Electrolytic conduction in solid salts. *Trans. Faraday. Soc.* **1938**, *34*, 485–499.

72 Zhang, K. H. L.; Walsh, A.; Catlow, C. R. A.; Lazarov, V. K.; Egdell, R. G. Surface Energies Control the Self-Organization of Oriented In$_2$O$_3$ Nanostructures on Cubic Zirconia. *Nano Lett.* **2010**, *10*, 3740–3746.

73 Walsh, A.; Catlow, C. R. A. Structure, stability and work functions of the low index surfaces of pure indium oxide and Sn-doped indium oxide (ITO) from density functional theory. *J. Mater. Chem.* **2010**, *20*, 10438–10444.

74 Walsh, A.; Da Silva, J. L. F.; Wei, S.-H.; Körber, C.; Klein, A.; Piper, L. F. J.; DeMasi, A.; Smith, K. E.; Panaccione, G.; Torelli, P.; Payne, D. J.; Bourlange, A.; Egdell, R. G. Nature of the band gap of In$_2$O$_3$ revealed by first-principles calculations and X-ray spectroscopy. *Phys. Rev. Lett.* **2008**, *100*, No. 167402.

75 Harvey, S.; Mason, T.; Körber, C.; Gassenbauer, Y.; Klein, A. Evidence for surface dipole modifications in In$_2$O$_3$-based transparent conductors. *Appl. Phys. Lett.* **2008**, *92*, 252106.

76 Krishnakumar, V.; Ramamurthi, K.; Klein, A.; Jaegermann, W. Band alignment of differently treated TCO/CdS interface. *Thin Solid Films* **2009**, *517*, 2558–2561.

77 Deuermeier, J.; Gassmann, J.; Brotz, J.; Klein, A. Reactive magnetron sputtering of Cu$_2$O: Dependence on oxygen pressure and interface formation with indium tin oxide. *J. Appl. Phys.* **2011**, *109*, No. 113704.

78 Soon, A.; Cui, X.-Y.; Delley, B.; Wei, S.-H.; Stampfl, C. Native defect-induced multifarious magnetism in nonstoichiometric cuprous oxide: First-principles study of bulk and surface properties of Cu$_2$O. *Phys. Rev. B* **2009**, *79*, No. 035205.

79 Soon, A.; Söhnel, T.; Idriss, H. Plane-wave pseudopotential density functional theory periodic slab calculations of CO adsorption on Cu$_2$O (111) surface. *Surf. Sci.* **2005**, *579*, 131–140.

80 Kramm, B.; Laufer, A.; Reppin, D.; Kronenberger, A.; Hering, P.; Polity, H. A.; Meyer, B. K. The band alignment of Cu$_2$O/ZnO and Cu$_2$O/GaN heterostructures. *Appl. Phys. Lett.* **2012**, *100*, No. 094102.

81 Walsh, A.; Da Silva, J. L. F.; Wei, S. H. Multi-component transparent conducting oxides: progress in materials modelling. *J. Phys.: Condens. Matter* **2011**, *23*, No. 334210.

82 Walsh, A.; Catlow, C. R. A.; Galvelis, R.; Scanlon, D. O.; Schiffmann, F.; Sokol, A. A.; Woodley, S. M. Prediction on the existence and chemical stability of cuprous fluoride. *Chem. Sci.* **2012**, *2*, 2565–2569.